

Observation of Tunable Band Gap and Two-Dimensional Subbands in a Novel GaAs Superlattice

G. H. Döhler, H. Künzel, D. Olego, K. Ploog, P. Ruden, and H. J. Stolz

Max-Planck-Institut für Festkörperforschung, D-7000 Stuttgart 80, Federal Republic of Germany

and

G. Abstreiter

Physik Department, Technische Universität München, 8046 Garching, Federal Republic of Germany

(Received 16 June 1981)

Luminescence and Raman measurements on a new type of superlattice consisting of n - and p -type doped GaAs layers grown by molecular-beam epitaxy confirm crucial predictions of theory. A strongly tunable energy gap is found in luminescence. Raman experiments provide the first observation of electronic subbands in purely space-charge-induced quantum wells. A combined analysis of the luminescence and Raman data yields excellent agreement with self-consistent subband calculations based only on the design parameters of the sample.

PACS numbers: 73.40.Lq, 78.55.Ds, 78.30.Gt

In this Letter we provide definite experimental evidence for the validity and applicability of basic ideas of a new type of artificial semiconductor superlattice which consists of ultrathin n - and p -type doped layers, possibly separated by intrinsic layers, of the same semiconducting material (" n - i - p - i " crystals).¹ Compared with the well-known compositional superlattices AlAs-GaAs² or InAs-GaSb³ these doped superlattices exhibit novel electronic properties which result from a very efficient spatial separation between electron and hole subbands (indirect gap in real space) by the periodic space-charge potential. This separation implies recombination lifetimes which may be increased by many orders of magnitude over those of bulk material. Consequently, large deviations of the electron and hole concentration from thermal equilibrium are metastable under weak excitation conditions. In addition, the space-charge-induced superlattice potential itself is strongly affected by a variation of the electron and hole concentration, e.g., by photoexcitation or carrier injection. The effective energy gap of a n - i - p - i crystal as well as the structure of the two-dimensional (2D) subbands should thus no longer be fixed material parameters but tunable quantities.

The n - i - p - i superlattice configuration used for the present investigations was grown by molecular-beam epitaxy.⁴ It consists of twenty n (Si) and p (Be) doped GaAs layers with equal doping concentrations $n_D = n_A = 1 \times 10^{18} \text{ cm}^{-3}$ deposited on a (100) semi-insulating substrate. The individual layer thickness is $d_n = d_p = 40 \text{ nm}$.

The concept of a tunable energy gap in this n - i -

p - i superlattice was first examined by photoluminescence (PL) measurements with the sample cooled to 4.2 K. Various laser lines of a Kr⁺-gas laser with either slit or point focus on the (100) surface of the sample were used as excitation source. Four PL spectra for $\lambda_L = 676.4 \text{ nm}$ as a function of the excitation intensity I^{exc} are shown in Fig. 1. For high I^{exc} the asymmetric PL spectrum approaches the direct-band-gap energy of GaAs. A strong redshift of about 200 meV is found with stepwise reduction of I^{exc} down to values of a few watts per square centimeter, where we reached the detectability limit of our experimental setup.

In order to obtain direct information on the expected quantization and subband structure in this GaAs n - i - p - i superlattice we additionally performed resonant inelastic light scattering experiments in backscattering geometry from the (100) surface of the sample. This technique has been

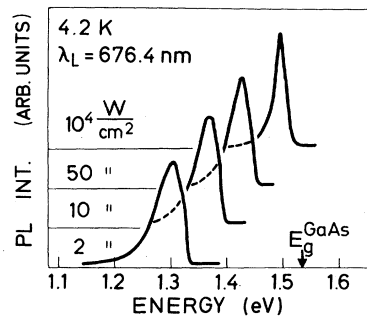


FIG. 1. Photoluminescence spectra of a GaAs n - i - p - i superlattice with $n_D = n_A = 10^{18} \text{ cm}^{-3}$ and $d_n = d_p = 40 \text{ nm}$ as a function of the laser excitation intensity.

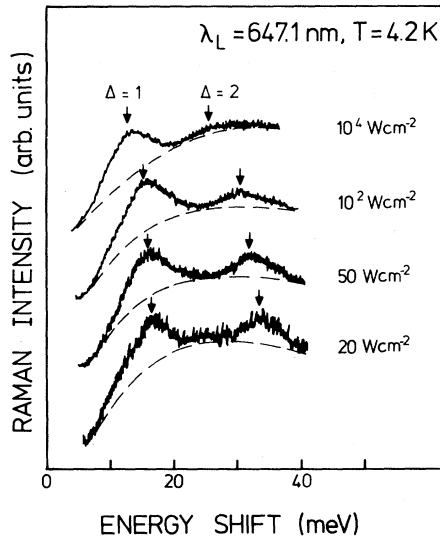


FIG. 2. Single-particle excitation spectra of the studied GaAs $n-i-p-i$ superlattice observed with resonant Raman scattering for different laser excitation intensities.

successfully applied to study the 2D subband structure in selectively doped $n-Al_xGa_{1-x}As/GaAs$ single heterojunction⁵ and multi-quantum-well structures.⁶ The bare single-particle intersubband excitation energies are measured by the spin-flip scattering signal which is polarized perpendicular to the exciting beam.⁷ The laser excitation line ($\lambda_L = 647.1$ nm) was chosen close to the $E_0 + \Delta_0$ gap of GaAs. The resonance condition is fulfilled for electrons in the conduction band but not for holes in the valence band. In Fig. 2 four Raman spectra obtained for different I^{exc} are shown. Two peaks sitting on top of the $E_0 + \Delta_0$ luminescence are clearly observed. These peaks are interpreted as single-particle intersubband transitions of the photoexcited electrons in the GaAs $n-i-p-i$ superlattice. With decreasing I^{exc} the peaks shift to higher energies.

We now show that the observed shift of the PL and the energetic position of the intersubband transitions, both as a function of I^{exc} , are in perfect quantitative agreement with theory. The only input data for our calculations are the design parameters n_D , n_A , d_n , and d_p of the GaAs $n-i-p-i$ superlattice investigated. The self-consistent potential $v_{sc}(z)$ seen by a carrier moving in the direction of periodic n - and p -type doping (z direction in Fig. 3) is the sum⁸ of a contribution $v_0(z)$ due to the bare ionized impurities, the Hartree term $v_H(z)$ of the mobile carriers, and an ex-

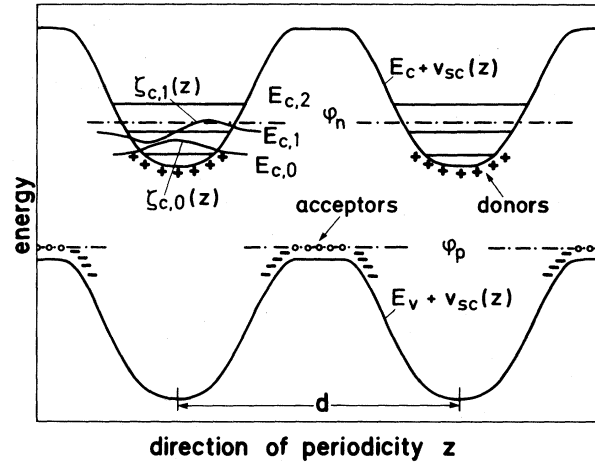


FIG. 3. Schematic real-space energy diagram of an $n-i-p-i$ crystal. See text for explanation.

change and correlation contribution $v_{xc}(z)$ which is treated in the local density approximation of the density functional formalism. At a given 2D electron concentration per layer $n^{(2)}$, the electron distribution $n(z)$ is obtained from $n(z) = \sum_{\mu} n_{\mu}^{(2)} \times |\zeta_{c,\mu}(z)|^2$. The subband wave functions $\zeta_{c,\mu}(z)$ are the self-consistent solutions of the effective-mass one-particle Schrödinger equation for conduction-band electrons in the potential $v_{sc}(z)$. The 2D-carrier concentration $n_{\mu}^{(2)}$ in the μ th subband is derived from the requirement of equal Fermi level φ_n in occupied subbands together with the condition $n^{(2)} = \sum_{\mu} n_{\mu}^{(2)}$. The hole distribution $p(z)$ is obtained to a good approximation by assuming that the holes populate a narrow impurity band above the valence subbands. This assumption corresponds to a cancellation of the acceptor space charge $-en_A(z)$ by holes within the central part of the p -type layers and vanishing $p(z)$ outside. The band edges modulated by the self-consistent potential $v_{sc}(z)$, the quasi Fermi levels φ_n and φ_p , the subband energies $E_{c,\mu}$, and the wave functions $\zeta_{c,\mu}(z)$ for the lower electron subbands in a $n-i-p-i$ superlattice are shown schematically in Fig. 3. The situation shown corresponds to an excited state of the crystal with $\varphi_n > \varphi_p$.

The results of the calculated electronic structure of the studied sample are summarized in Fig. 4 and compared with experiments. Figure 4(a) displays the calculated subband energies $E_{c,\mu}$ and the electron quasi Fermi level φ_n as a function of carrier concentration in the range $n^{(2)} = (1.5-4.0) \times 10^{12} \text{ cm}^{-2}$. The hole quasi Fermi level φ_p is assumed to lie in the center of the

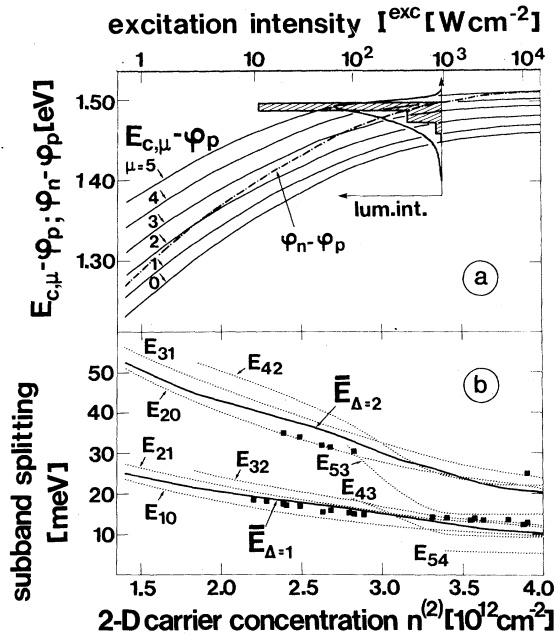


FIG. 4. Variation of the energy gaps $E_{c,\mu} - \varphi_p$ and of $\varphi_n - \varphi_p$ (top part) and of subband spacings $E_{\mu\nu} = E_{c,\mu} - E_{c,\nu}$ (dotted lines in bottom part) vs carrier density per layer as calculated self-consistently for the sample investigated. Inset in top part: Comparison of calculated spectrum (shaded area) with the observed one ($\lambda_L = 799.9 \text{ nm}$) (full line). Bottom part: squares, single-particle intersubband energies as determined by Raman spectroscopy; heavy lines, calculated average subband spacings.

narrow acceptor impurity band and is taken as the origin of the energy scale. The strong increase of the energy gap $E_{c,0} - \varphi_p$ reflects the decrease of the amplitude of the self-consistent space-charge potential $v_{sc}(z)$ due to increasing compensation of the bare impurity space-charge potential $v_0(z)$ by the mobile carrier potential $v_H(z) + v_{xc}(z)$.

The luminescence of the GaAs *n-i-p-i* superlattice arises from recombination of electrons in the occupied conduction subbands with the holes in the impurity band. The spectral range of photon energies is $E_{c,0} - \varphi_p < \hbar\omega < \varphi_n - \varphi_p$. The relative intensities of the contributions of different subbands, however, increases strongly with the index μ because of exponentially increasing overlap between electron and acceptor band wave functions. Therefore, an asymmetric, stair-shaped luminescence spectrum is expected. As an example the calculated spectrum is shown for $n = 3.4 \times 10^{12} \text{ cm}^{-2}$ as an inset in Fig. 4(a).

The total PL is expected to increase with $n^{(2)}$,

also on an exponential scale, because of the increasing overlap between electron and hole states when $v_{sc}(z)$ flattens (see Fig. 3). Together with the stationarity condition it follows that the steady-state PL exhibits a roughly logarithmic blue shift as a function of increasing I^{exc} . The high-energy edge of the experimental PL spectrum $\hbar\omega_{\text{max}}$ at a given I^{exc} yields the value of $\varphi_n - \varphi_p$. In terms of our calculated results of Fig. 4(a) the observed shift of the high-energy edge of the PL between $\hbar\omega_{\text{max}} = 1.28$ and 1.51 eV corresponds to a variation of the steady-state 2D carrier concentration between $n^{(2)} = 1.46 \times 10^{12}$ and $3.80 \times 10^{12} \text{ cm}^{-2}$. The relation between I^{exc} , PL frequencies, and steady-state carrier concentration was used to calibrate the carrier-concentration scale with the experimental I^{exc} scale (see top scale in Fig. 4). Indeed, a roughly logarithmic relation between those two scales is found.

For a comparison between the shape of the experimentally observed and the theoretical spectra the experimental PL spectrum obtained with the 799.9 nm laser line is shown in the inset of Fig. 4(a). The theoretically expected steplike structure is not observed, but the width and the asymmetric shape agree quite well with the theory. The lack of the steplike structure is easily understood as a consequence of inhomogeneous excitation of different *n-i-p-i* layers caused by the limited penetration depth of the laser light. The excitation intensity decreases by about a factor of 2 within the *n-i-p-i* structure. Therefore, the steady-state carrier concentration and, hence, the PL energies decrease slightly from layer to layer. In the total spectrum, which is the superposition of all these contributions, the steplike structure can no longer be detected.

For the detection of quantization effects in a *n-i-p-i* crystal inelastic light scattering experiments are particularly suitable for several reasons. Inspection of Fig. 4(b) shows that the intersubband spacing $E_{c,\mu+\Delta} - E_{c,\mu}$ for $\Delta = 1$ and 2 is much less sensitive to changes of $n^{(2)}$, and thus to inhomogeneous excitation, than the gap energies $E_{c,\mu} - \varphi_p$. In addition, the contributions of only a few *n*-type layers near the surface are heavily weighted because the scattered light is strongly absorbed if the photon energy is close to the $E_0 + \Delta_0$ gap of GaAs. Finally, the (nearly) momentum-independent energy differences $E_{c,\mu+\Delta} - E_{c,\mu}$ causing a (broadened) line spectrum are more easily detected than a steplike structure in the luminescence.

In Fig. 4(b) we have plotted the observed subband splitting as a function of steady-state carrier concentration which was determined from the simultaneously measured PL signal. The full lines in Fig. 4(b) correspond to the average subband spacing $\bar{E}_{\Delta=1}$ and $\bar{E}_{\Delta=2}$ obtained by weighting with the number of states participating in the respective $E_{c,\mu+\Delta} - E_{c,\mu}$ processes. The excellent quantitative agreement between the measured and the calculated intersubband spacing, even over a wide range of carrier concentration, leads unambiguously to the conclusion that the photoexcited electrons in the GaAs $n-i-p-i$ superlattice are populating 2D subbands.

The results of the photoluminescence and the Raman measurements confirm the most crucial predictions of the theory of $n-i-p-i$ superlattices.¹ The observation of a strong shift of the luminescence as a function of excitation intensity demonstrates that introducing the concept of a tunable indirect energy gap in real space is sound and that even large nonequilibrium carrier concentrations are metastable. Inelastic light scattering definitely shows single-particle intersubband excitations. This result is of special significance as it represents the first observation of quantization and 2D-subband formation in purely space-charge-induced potential wells. It proves, in particular, that the statistical impurity potential fluctuations are so effectively screened by the mobile electrons that they do not prevent the formation of 2D subbands. Excellent quantitative agreement of the observed variation of effective energy gap and corresponding subband spacing

with self-consistent calculations of the $n-i-p-i$ subband structure is found over the full range of carrier concentrations studied. The agreement between theory and experiment demonstrates not only that our theoretical approach is correct, but it also proves a high standard of controlled doping with sharp profiles accomplished by molecular-beam epitaxy.

We would like to acknowledge the expert help in sample preparation of A. Fischer and the technical assistance of H. Hirt and M. Siemers. This work was supported in part by the Bundesministerium für Forschung und Technologie of the Federal Republic of Germany.

¹G. H. Döhler, Phys. Status Solidi (b) **52**, 79, 533 (1972), and J. Vac. Sci. Technol. **16**, 851 (1979).

²See, for example, R. Dingle, in *Festkörperprobleme: Advances in Solid State Physics*, edited by H. J. Queisser (Vieweg, Braunschweig, 1975), Vol. XV, p. 21; L. Esaki and L. L. Chang, Thin Solid Films **36**, 285 (1976).

³L. L. Chang and L. Esaki, Surf. Sci. **98**, 70 (1980).

⁴K. Ploog, A. Fischer, G. H. Döhler, and H. Künzel, in *Gallium Arsenide and Related Compounds 1980*, Institute of Physics Conference Series No. 56, edited by H. W. Thim (Institute of Physics, London, 1981), p. 721.

⁵G. Abstreiter and K. Ploog, Phys. Rev. Lett. **42**, 1308 (1979).

⁶A. Pinczuk, H. L. Störmer, R. Dingle, J. M. Worlock, W. Wiegmann, and A. C. Gossard, Solid State Commun. **32**, 1001 (1979).

⁷E. Burstein, A. Pinczuk, and D. L. Mills, Surf. Sci. **98**, 451 (1980).

⁸G. H. Döhler, Surf. Sci. **73**, 97 (1978).